

Classification

Physics Abstracts

61.16D — 61.70T — 61.80

## Cross-sectional electron microscopy investigation of silicon amorphisation during high temperature zinc-ion bombardment

Joël Faure, Stephan Simov(\*), Maria Kalitzova(\*), Gérard Balossier, Lalit-Mohan Bharadwaj(\*\*), Alain Claverie(\*\*\*) and Pierre Bonhomme

Laboratoire de Microscopie Electronique, INSERM U314, 21 rue Clement Ader, 51100 Reims, France

(Received March 20, 1990; accepted June 29, 1990)

**Résumé.** — L'amorphisation d'un substrat monocristallin de silicium par implantation, à 110 °C, d'ions  $Zn^{+}$  de 120 keV a été étudiée par microscopie électronique "sur la tranche". Le calcul de l'énergie reçue par la cible en collisions nucléaires (énergie de dommage) a permis d'utiliser le modèle de la "densité critique d'énergie de dommage" pour la transition cristal  $\rightarrow$  amorphe du silicium implanté. La confrontation des résultats théoriques aux mesures expérimentales de l'épaisseur des couches amorphes, obtenues pour différentes doses implantées, conduit à une valeur critique de  $10 \text{ eV} \cdot \text{at}^{-1}$  pour la densité d'énergie de dommage associée à l'amorphisation du silicium. La nécessité de densités d'énergie de dommage supérieures à cette valeur critique, aux premiers stades de l'amorphisation, peut être reliée à un taux de recombinaison important des défauts ponctuels, lié à la température d'implantation de 100 °C. Par ailleurs, lorsque la dose implantée augmente, la rugosité de l'interface amorphe/cristal diminue au fur et à mesure de sa progression vers la profondeur, ce qui traduit une homogénéisation du processus d'endommagement de la cible. Enfin, malgré la température d'implantation utilisée, aucune recristallisation notable, liée à un recuit dynamique, n'a été observée.

**Abstract.** — Cross-sectional transmission electron microscopy has been applied to the characterisation of silicon amorphisation due to  $Zn^{+}$  (120 keV) ion bombardment at 110 °C. In spite of the implantation temperature used, we did not notice any annealing effect. This point is discussed in light of the low ion current density used in these experiments and experimental results arising from literature. Calculations of the energy received by the target through nuclear collisions (i.e. damage energy) have been recombined with concepts arising from the "critical damage energy density" model for the crystal to amorphous transition of silicon. Comparison of the experimental measurements of the extension of the amorphous layer for increasing doses with the theoretical calculations shows that a damage energy density of about  $10 \text{ eV} \cdot \text{at}^{-1}$  is required for silicon amorphisation. It is suggested that temperature effects are responsible for the need of higher damage energy density to produce a first continuous amorphous layer than to extend this layer to greater depth. The experimental observations clearly show that the roughness of the amorphous-crystalline interface is reduced

---

(\*) *Permanent address:* Institute of Solid State Physics, Bulgarian Academy of Sciences, Sofia 1784, Bulgaria.

(\*\*) *Permanent address:* Central Scientific Instruments Organisation, Chandigarh 160020, India.

(\*\*\*) *Permanent address:* Centre d'Elaboration des Matériaux et d'Etudes Structurales, 31055 Toulouse, France.

when increasing the ion dose, and hence its depth location ; which suggest that the damage process becomes more homogeneous.

## 1. Introduction.

Zinc implantation in silicon has been the subject of different investigations [1 – 7] . Due to its low solubility in silicon,  $Zn^{+}$  implantation can produce strongly supersaturated surface layers [1] and the segregation of zinc impurities is used as in marker explosive crystallisation occurring during pulse laser annealing [2 – 4] . Moreover, the use of zinc as a dopant reveals some interest in optoelectronic devices fabrication such as photoresistors, light amplifiers, photodiodes etc. [5, 6]. Recently, zinc implantation has received a new attention in thermal oxidation of silicon [7] . Oxidation kinetics have been found to be strongly correlated to zinc segregation at the oxide-silicon interface and to the nature of the ion induced damage which is stable at the oxidation temperature.

Nevertheless, the structural modifications induced in a monocrystalline silicon substrate during high dose zinc implantation has been very less studied.

The aim of this paper is to report results on the formation and extension of an amorphous layer due to 110 °C/120 keV  $Zn^{+}$  bombardment in silicon. Cross-sectional transmission electron microscopy (XTEM) has been used for the characterisation of damage accumulation for increasing doses, as well as the interfacial roughness of the amorphous surface layers, for which RBS experiments are very difficult to perform. The structure of the crystalline/amorphous (c/a) interface has been investigated with lattice imaging observations. We successfully compared the experimental results with the prediction of the F.F. Morehead and B.R. Crowder's model [8] .

Calculations were performed to provide a theoretical support to the XTEM observations, by the use of the Lupin program of Vieu *et al.* [9] . This program gives accurate depth distributions of the energy received by the silicon target through nuclear collisions, called damage energy. The damage energy calculations and the experimental results have been combined with concepts from the “critical damage energy density” (CDED) model for the crystal to amorphous transition (c → a) [10] . Finally the influence of the implanted dose on the interfacial roughness of the c/a interface and the effect of the temperature have been discussed.

## 2. Experiments.

(111) oriented silicon wafers (n type ;  $2\text{-}5 \text{ Ohm.cm}^{-1}$ ) of standard integrated circuit quality were implanted with  $Zn^{+}$  ions at an energy of 120 keV and doses from  $10^{13}$  to  $10^{16}$  ions. $\text{cm}^{-2}$ . During irradiation the target was mounted on a resistively heated copper block, the temperature of which was monitored by a thermocouple. The silicon target has been heated to 110 °C during  $Zn^{+}$  implantation. Channeling effects were minimized by using a beam incidence of 7-8° off the surface normal. Ion current densities less than  $3 \mu\text{A.cm}^{-2}$  were used so that no additional heating of the silicon sample occurs during ion implantation.

For XTEM observations, samples were prepared without any pre-surface treatment to avoid modifications of the implanted surface. During mechanical preparation, care was taken to maintain  $\langle 110 \rangle$  azimuth perpendicular to the sample surface. Final thinning of the specimen was done by 3-5 keV  $Ar^{+}$  ion beam at a shallow angle (10-15°) of beam incidence with low current density ( $3 \mu\text{Acm}^{-2}$ ) . The thinned specimen were directly observed under Philips CM30 electron microscope.

The depth and extent of the amorphous layers were investigated by mean of Bright Field (BF) images. Different 220 Dark Field (DF) were performed to check the crystalline or amorphous structure of the material. Lattice imaging was finally used to study the amorphous-crystalline interface.

### 3. Experimental results.

Figure 1 presents a set of XTEM micrographs showing the effect of  $Zn^+$  implantation. In all micrographs the silicon surface is shown with an arrow.

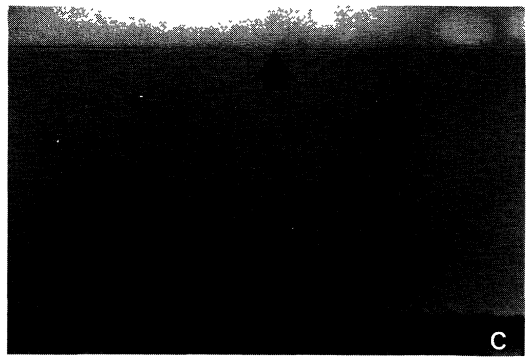
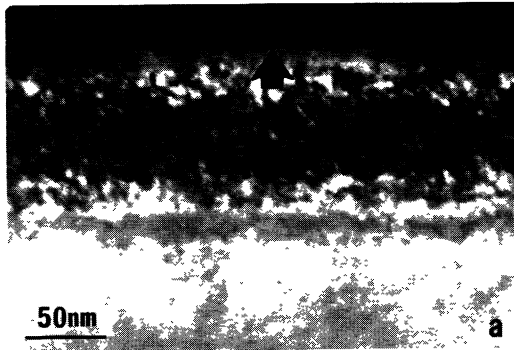


Fig. 1. — Cross-sectionnal TEM images of the creation and extension of an amorphous silicon layer ((111) initial orientation) at 110 °C for increasing doses of 120 keV  $Zn^+$  ions. (a)  $10^{14}$  ions.cm<sup>-2</sup> ; (b)  $10^{15}$  ions.cm<sup>-2</sup> ; (c)  $10^{16}$  ions.cm<sup>-2</sup>. (a) and (b) are DF images while (c) is a BF one. The arrows point to the silicon surface covered by the epoxy glue.

At a dose of  $10^{13}$  ions.cm<sup>-2</sup>, DF observations and microdiffraction experiments failed to reveal the presence of amorphous material.

In figure 1a, associated with a  $10^{14}$  ions.cm<sup>-2</sup> dose, the 220 DF image reveals a buried non-crystalline layer (black layer in figure) lying from about 30 to 85 nm from the silicon surface. Mi-

crodiffraction patterns revealed the two diffuse rings proving the amorphous nature of this layer. At this stage, the interfacial roughness is high (20 nm) both in the upper and lower regions of the layer, and the surface consists of crystallites and amorphous pockets.

Increasing the dose up to  $10^{15}$  ions.cm<sup>-2</sup> (Fig. 1b) results in the extension of the amorphous layer up to the surface and to a depth of 150 nm. This DF image shows clearly that, at this stage, the amorphous layer is strongly homogeneous without any crystallites even close to the silicon surface. Further increasing on the implantation dose to  $10^{16}$  ions.cm<sup>-2</sup> (Fig. 1c) leads to a slow extension of this continuous amorphous layer to a depth of about 175 nm.

From this set of XTEM micrographs, it is clearly showed that, as the dose is increased, the extension of the amorphous layer proceeds at a reduced rate while the interfacial roughness is lowered : in the b and c micrographs, the c/a interface is very smooth. The lattice image of figure 2 illustrates the atomic roughness of the c/a interface for the  $10^{15}$  ions.cm<sup>-2</sup> implanted sample. The interfacial region appears atomically sharp. The roughness of the interface is small over the whole implanted layer and the experimental dispersion in the c/a interfacial depth position is less than 7 nm. So, at this depth, the amorphisation process becomes strongly homogeneous.

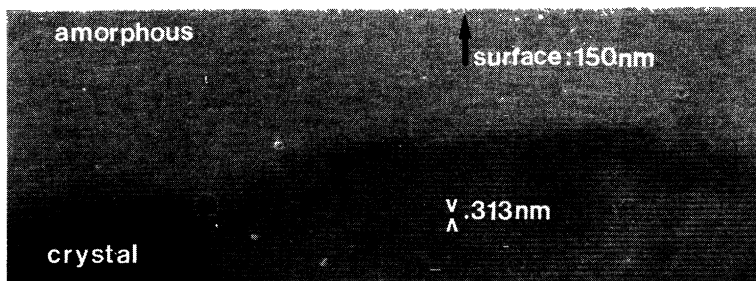


Fig. 2. — Cross-sectionnal image of the c/a interface for a  $10^{15}$  ions.cm<sup>-2</sup> dose of 120 keV Zn<sup>+</sup> incident on a (111) silicon substrate at 110 °C. The interfacial roughness is less than 7 nm over the whole implanted layer.

Moreover, the lattice fringes characteristic of monocrystalline material are sharply interrupted at the c/a interface without any extended defects. So, at the implantation temperature of 110 °C, no dynamic annealing effect is visible : indeed, when the induced recrystallization proceeds along the (111) direction the resulting silicon substrate is always highly twinned [11 – 13] ; and so easy to identify in the lattice imaging mode.

#### 4. Discussion.

The temperature dependence of the critical dose required to produce a continuous amorphous layer for the Zn<sup>+</sup>/Si system, is presented, on a logarithmic scale, in figure 3. This curve is deduced from the F.F. Morehead and B.R. Crowder's model [8], in which the influence of temperature is interpreted in terms of thermal diffusion of vacancies. This model predicts that silicon amorphisation is possible up to 300 °C, and at 110 °C the calculated amorphisation dose is about  $6 \times 10^{14}$  ions.cm<sup>-2</sup>. There is a good agreement between this model and the experimental results : XTEM micrographs 1a and 1b clearly show that the dose needed to produce a first continuous amorphous layer is between  $10^{14}$  and  $10^{15}$  ions.cm<sup>-2</sup>.

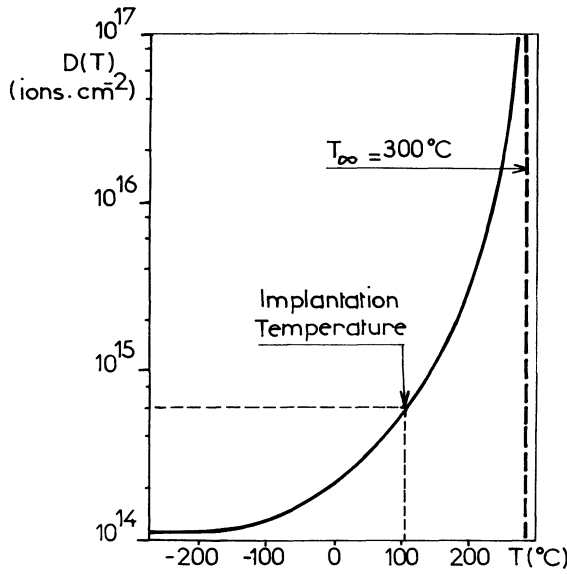


Fig. 3. — Temperature dependence of the critical Zn<sup>+</sup> dose needed to produce a continuous amorphous silicon layer from the F. F. Morehead and B. L. Crowder's model [8].  $D(T) = D_0 \times \left(1 - K' \times (dE/dx)^{-1/2} \times \exp(-E_{df}/2kT)\right)^{-2}$   $D_0 = 1.14 \times 10^{14}$  ions.cm<sup>-2</sup> : amorphisation dose in the absence of vacancy outdiffusion (at 0 K).  $K' = 364 \times 10^3$  (eV.cm<sup>-1</sup>)<sup>1/2</sup> : adjustable parameter depending on the implanted substrate.  $(dE/dX)_0 = 1.1 \times 10^{10}$  eV.cm<sup>-1</sup> : energy-independent nuclear stopping power deduced from an approximation of the Nielson equation (8).  $E_{df} = 0.12$  eV : activation energy, for vacancy diffusion.  $k = 8.5 \times 10^{-5}$  eV.K<sup>-1</sup> : Boltzmann constant.

The damage energy depth distribution for the Zn<sup>+</sup> (120 keV)/Si system obtained with the Lupin program [9], is presented in figure 4. This program is an extension of the theory of Brice [14], which takes into account the energy transported by the recoiling atoms created along the ion path. So, the Lupin code gives accurate distribution of the damage energy, which could be favourably compared with Monte Carlo simulations [15] as well as experimental results [9]. The depth corresponding to the maximum damage energy lies in the 55-65 nm range, which agrees well with the central part of the first continuous buried layer from figure 1a. The curve appears to be mainly Gaussian in shape and tends to zero at a depth close to 180 nm.

The CDED model proposed earlier by Stein *et al.* [10] has recently received more attention through the works of Narayan *et al.* [16], Claverie *et al.* [17, 18] and many other authors, and permits a quantitative approach to the crystalline to amorphous transition. According to this model, a crystal which contains a sufficiently high concentration of defects will relax into the amorphous state. Since it is commonly assumed that for metals and semiconductors, the defect concentration is related to the amount of nuclear energy loss received by the target, a critical defect density, related to the c→a transition, is then associated to a "critical damage energy density" (CDED), noted  $E_{dc}$  and defined by :

$$E_{dc} = \frac{\Phi_c(z) * E_d(z)}{\rho} \quad (1)$$

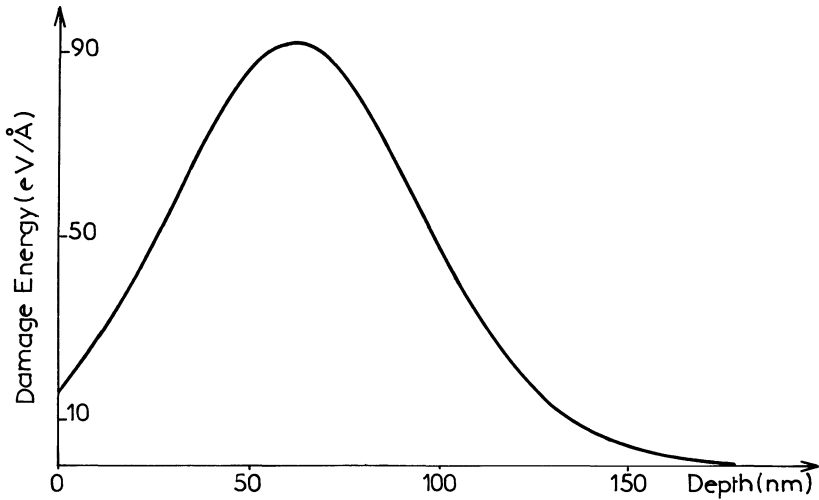


Fig. 4. — Damage energy distribution for 120 keV  $\text{Zn}^+$  on silicon from the Lupin program (9) obtained with the following parameters : mean projected range :  $R_p = 93.8 \text{ \AA}$  ; standard deviation in the projected range :  $S_p = 33.4 \text{ \AA}$ .

where  $\Phi_c(z)$  ( $\text{ions.cm}^{-2}$ ) is the dose needed to amorphise the crystal at the depth  $z$  ;  $E_d(z)$  ( $\text{eV.}\text{\AA}^{-1}$ ) is the value of the damage distribution at the same depth and  $\rho$  is the atomic density of the silicon target ( $5 \times 10^{22} \text{ at.cm}^{-3}$ ), then the CDED value  $E_{dc}$  is in electron volt per atom. We have reported in figure 5 the depth of the  $c/a$  interfaces as a function of  $\text{Zn}^+$  dose, on a logarithmic scale. The width of the experimental bars represents the maximum interfacial roughness detected on the XTEM micrographs. When the interfacial roughness is high (Fig. 1a), the position of the interface corresponds to the middle of the rough interface. This type of representation, called a dose-depth phase diagram, is readily adapted to the determination of the  $E_{dc}$  value : indeed, a curve deduced from relation (1) on the basis of our calculations (Fig. 4) and assuming a  $E_{dc}$  value of  $10 \text{ eV.at}^{-1}$  offers the best fit to the experimental results. This curve clearly confirms that a dose of  $10^{13} \text{ ions.cm}^{-2}$  is insufficient for the formation of a first amorphous layer, as suggested by the experimental observations.

Nevertheless, this agreement is clearly better for higher doses than for lower ones. In the vicinity of the damage peak, the damage energy loss per ion is high (see in Fig. 4) so that, denser cascades develop. So, for low doses the damage process is less statistical (resulting in a high dispersion of the damaged region). Thermal diffusion of the point defects from the core of denser cascades, resulting in a high level of recombination, is responsible of the increasing in the experimental amorphisation doses in comparison with the theoretical ones. In the deeper regions, the damage energy loss per ion is low and most of cascades are less dense than around the peak region. An increasing number of ionic impacts (i.e. cascade overlapping) is necessary to reach the critical defect density needed for the  $c \rightarrow a$  transformation. The damage process is then more homogeneous, resulting in the smoothing of the  $c/a$  interface during its progression for increasing doses, as earlier proposed by Claverie *et al.* [17].

Concurrently, we observed a reducing in the extension speed of the amorphous layer. The dose dependence of damage accumulation has been discussed recently by Holland *et al.* [19].

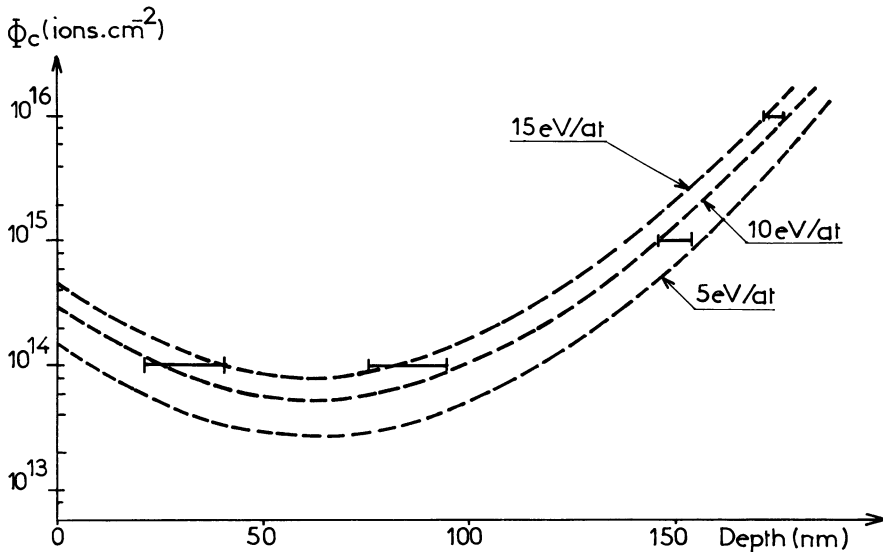


Fig. 5. — Dose/Depth phase diagram of the 120 keV- $Zn^+$ /Si – 110 °C implantation system. The bars indicate the experimental measurements. The curves present the prediction of the CDED model at different  $E_{dc}$  values.

They related the initial acceleration of the c- $\rightarrow$ a transition to a sudden increase in the divacancy concentration due to a high trapping interstitial type defects by the amorphous phase.

## 5. Conclusions.

XTEM has been used for the study of the formation and extension of a silicon amorphous layer of about 200 nm, due to  $Zn^+$  implantation and comparison with specific damage energy calculations has been performed.

Fitting experimental results from the  $Zn^+$  (120 keV)/Si(110 °C) system with concepts arising from the CDED model, leads to a value of about  $10 \text{ eV}\cdot\text{at}^{-1}$  for the c  $\rightarrow$  a transformation to occur. This energy density value, which agrees well with previous experimental works [15, 17, 20], is representative of an “intermediate” ion according to the Lindhard-Scharff-Schiott description [21]. Nevertheless, this damage energy density is not enough to produce a first buried amorphous layer; which can be related to a high thermal diffusion, at the implantation temperature of 110 °C, of point defects resulting in a high level of recombination.

This XTEM study also clearly shows that the roughness of the c/a interface reduces when increasing the ion dose. We suggest that this reduction is related to an increasing in the number of ionic impacts (i.e. cascade overlapping) necessary for the c  $\rightarrow$  a transition, so that the damage process becomes more homogeneous.

## Acknowledgements.

We thank Miss L. Kilian for the careful specimen preparation and Mr S. Lebonvallet for his informatic help.

## References

- [1] CULLIS A. G., WEBER H. C., POATE J. M. and CHEW N. G., *J. Microsc.* **118** (1980) 41.
- [2] ERYU O., MURAKAMI K., TAKITA K. and MASUDA K., *Nucl. Instrum. Methods Phys. Res.* **B33** (1988) 665.
- [3] MUSTAFIN T. N., KACHURIN G. A., POPOV V. P., PRIDACHIN N. B., SERYAPIN V. G. and SMIRNOV L. S., *Sov. Phys. Semicond.* **12** (1978) 776
- [4] MUSTAFIN T. N., POPOV V. P., SERYAPIN V. G. and SMIRNOV L. S., *Sov. Phys. Semicond.* **16** (1982) 75.
- [5] KORNILOV B. V., Physics of p-n junctions and semiconductor devices (Ryakin and Shmartsev, London) 1971, p. 350.
- [6] PETRUNINA G. E. and SHOPEN V. I., *Sov. Phys. Semicond.* **9** (1975) 383.
- [7] HOLLAND O. W., WHITE C. W. and PENNYCOOK S. J., *J. Mater. Res.* **3** (1988) 898.
- [8] MOREHEAD Jr. F. F. and CROWDER B. L., *Radiat. Eff.* **6** (1970) 27.
- [9] VIEU C., CLAVERIE A., FAURÉ J. and BEAUVILLAIN J., *Nucl. Instrum. Methods Phys. Res.* **B28** (1987) 229.
- [10] STEIN H. J., VOOK F. L., BRICE D. K., BORDERS J. A. and PICRAUX S. T., Proceedings of the First International Conference on Ion Implantation (Gordon and Breach, London) 1971, p. 17.
- [11] BERTI M., BRIGO A. V., LULLI G., MERLI P. and VITTORI ANTISARI M., *Phys. Status. Solidi* (a) **94** (1986) 95.
- [12] CSEPREGI L., MAYER J. W. and SIGMON T. W., *Appl. Phys. Lett.* **29** (1976) 92.
- [13] CULLIS A. G., SEIDER T. E. and MEEK R. L., *J. Appl. Phys.* **49** (1978) 5188.
- [14] BRICE D. K., *J. Appl. Phys.* **B46** (1975) 385.
- [15] VIEU C., Thesis, University of Toulouse (1987).
- [16] NARAYAN J., FATHY D., OEN O. S. and HOLLAND O. W., *J. Vac. Sci. Technol.* **A(2)** (1984) 1303.
- [17] CLAVERIE A., VIEU C., FAURÉ J. and BEAUVILLAIN J., *J. Appl. Phys.* **64** (1988) 4415.
- [18] CLAVERIE A., VIEU C., FAURÉ J. and BEAUVILLAIN J., *Mater. Sci. Eng.* **B2** (1989) 99.
- [19] HOLLAND O. W., PENNYCOOK S. J. and ALBERT G. L., *Appl. Phys. Lett.* **55** (1989) 2503.
- [20] THOMPSON D. A., *Radiat. Eff.* **56** (1981) 105.
- [21] LINDHARD J., SCHARFF M. and SCHIOTT H., *Mat. Fys. Medd. Dan Vid. Selsk* **33** (1963) 1.

Cet article a été imprimé avec le Macro Package "Editions de Physique Avril 1990".